 doi:10.20944/preprints202209.0452.v1

Article

Demystifying the Preventive Measures for Flooding from Groundwater Triggered by the Rise in Adjacent River Stage

Raaghul Kumar [1], Munshi Md. Shafwat Yazdan[1,*] and Md Abdullah Al Mehedi[2]

[1] Civil & Environmental Engineering, Idaho State University, Pocatello, ID 83209, USA; raaghulkumar@isu.edu
[2] Department of Civil and Environmental Engineering, Villanova University, Villanova, PA 19085, USA; mmehedi@villanova.edu
* Correspondence: yazdmuns@isu.edu; Tel.: +1-208-240-7480

Abstract: Groundwater (GW) flooding mechanisms differ from river flooding both spatially and temporally, and preventative methods against groundwater flooding must take this into account. Although groundwater flooding caused by river water rise occurs seldom, it can occasionally become severe and last for a long time if the river is significantly flooded. In the southwest portion of the research domain, Friedrichshafen with a few urban communities, the level of the groundwater table was discovered to be roughly 1 m below the surface. It was discovered that the urban settlement area only has one-story buildings. In the study region, it is typical for the single-story building's foundation bottom level to extend up to a depth of about 1.5 meters. Therefore, flood mitigation methods are taken into account for the southwest portion of the study region. The installation of a pumping well, drainage, and a barrier in the affected area are three different flood control strategies that are taken into consideration for the study area. From a technical and cost-benefit perspective, installing a pumping well that withdraws water and lowers the groundwater table was found to be the most effective flood control measure locally in a small region (e.g., 1km x 1km). By contrast, removing groundwater by building drainage and barriers was also shown to be ineffective to lower the groundwater table over an extended region and was significantly more expensive than the installation of wells. Additionally, when river flooding is taken into account compared to the default scenario where no intake of water from the river is included along the western border of the study area, it is discovered that the spread of pollution is significantly greater.

Keywords: Flooding from Groundwater; FEFLOW; Groundwater Modelling; Rise in River stage; Super Mesh

1. Introduction

One of the major reasons of groundwater flooding is the result of river water rise [1, 5]. This tends to occur after considerable period of sustained high rainfall [6-8]. Groundwater flooding may initially be invisible as underground flooding. Flooded basements are an early sign of groundwater flooding [9-10]. As the water level rises the water may emerge above the ground level causing flooding of buildings, roads and farmland [11-13]. Groundwater flooding can persist for weeks after river waters have receded [14-18]. In addition to rising into man-made ground, such as basements and other subsurface infrastructure, groundwater flooding also refers to the emergence of groundwater at the ground surface away from perennial river systems [19]. When the normal ranges of groundwater level and groundwater flow are exceeded, the effects of groundwater flooding can be severe. Since it was added to the EU Floods Directive (2007/60/EC), groundwater flooding risk has drawn increased attention in Europe. The Directive, which went into effect in November 2007, has rules for evaluating the risk of groundwater flooding, creating groundwater flood hazard maps, and putting in place measures to manage any major risk [20]. Following significant groundwater flooding incidents over the previous ten years, groundwater has now been included in the Directive. In places of Chalk outcrop

 doi:10.20944/preprints202209.0452.v1

and in the flood plains of significant rivers, the effects of groundwater flooding have been particularly severe. When heavy rainfall is combined with antecedent conditions of high groundwater levels and high unsaturated zone moisture content, groundwater flooding occurs in Chalk catchments. Increases in spring and stream base flow as well as the reactivation of dormant springs in dry valleys far from perennial stream channels can all result from groundwater level elevations of up to tens of meters. High groundwater levels kept stable by protracted periods of drainage from the unsaturated zone cause flooding to frequently last longer than necessary [21]. Examples include the Somme Valley and the floods that occurred in southern England in 2000 and 2003 [22].

The location, timing, and severity of groundwater flooding can be significantly impacted by the topographical changes to flood plains brought on by urbanization. As a result, risk evaluation may become quite difficult. Finding strategies to lower the likelihood of groundwater flooding as part of comprehensive flood risk management plans is difficult. The motivation of the study is to analyze the groundwater flooding due to rise of river water level, to identify the spread of contamination due to flooding and to outline the suitable mitigation measures for flooding. Moreover, Quality analysis of the model as well as sensitivity analysis for some parameters also fall into the goals of the study. This paper focuses on groundwater flooding in major river flood areas. The objective of the study is to explore the prevention techniques of groundwater flooding due to river water rise in urban setting, the spread of contamination and to strategize the suitable mitigation measures for flooding using FEFLOW.

2. Materials and Methods

The groundwater problem can be described by the set of differential equations for flow balance in the model domain and at the boundary of the model domain [23-27].

$$\frac{\partial}{\partial x_1}\left[k_{11}\frac{\partial h}{\partial x}\right]+\frac{\partial}{\partial x_2}\left[k_{22}\frac{\partial h}{\partial x_2}\right]+w=s_s\frac{\partial h}{\partial t} \quad (1)$$

K_{ii} (m/s) is hydraulic conductivity along xi coordinate i = 1,2, h is hydraulic head, w is volumetric flux (source/sink term), Ss is specific storage of the soil material (porous material), x1, x2 are the Cartesian coordinates, and t being time coordinate. For 2D problems with constant hydraulic conductivity in each coordinate direction the equation can be simplified to

$$k_{11}\frac{\partial^2 h}{\partial x_1^2}+k_{22}\frac{\partial^2 h}{\partial x_2^2}+w=s_s\frac{\partial h}{\partial t} \quad (2)$$

For steady groundwater flow the equation can be simplified to

$$k_{11}\frac{\partial^2 h}{\partial x_1^2}+k_{22}\frac{\partial^2 h}{\partial x_2^2}+w=0 \quad (3)$$

Boundary conditions can be h = h0 i.e., Dirichlet boundary condition with given head, q = qB i.e., Neumann boundary condition with given flux and q = f(h) i.e., Cauchy boundary condition with flux depends on the head [28-32]. Finite element method is used to discretize the differential equation in Feflow [33-34]. A direct frontal solver can be used to resolve the set of linear algebraic equations that result from the typical Galerkin approximation. The Picard iterative technique with options for relaxation is used to solve the nonlinear algebraic equations that come from coupled instances [35–42]. Time is discretized using a straightforward finite difference algorithm.

2.1. Study Area

Near Friedrichshagen, a little German town in the southeast of Berlin, nitrate contamination has been found. Two water supply wells have an increasing concentration [23–24]. There are two possible places where the contamination came from: The first is a group of desolate sewage fields near a wastewater treatment facility in an industrial area northeast of town. Further east is an abandoned trash disposal plant, which is the other potential source. To assess the overall risk to groundwater quality and to calculate the possible

 doi:10.20944/preprints202209.0452.v1

pollution, a three-dimensional groundwater flow and pollutant transport model is set up. The town is surrounded by many natural flow boundaries, such as rivers and lakes (Figure 1). There are two small rivers that run NorthSouth on either side of Friedrichshagen that can act as the eastern and western boundaries. The lake Müggelsee can limit the model domain to the south. The northern boundary is chosen along a northwest-southeast hydraulic contour line of groundwater level north of the two potential sources of the contamination. [35-39]. The geology of the study area is comprised of Quaternary sediments. The hydrogeologic system contains two main aquifers separated by an aquitard. The top hydrostratigraphic unit is considered to be a sandy unconfined aquifer up to 7 meters thick. The second aquifer located below the clayey aquitard has an average thickness of approximately 30 meters. The northern part of the model area is primarily used for agriculture, whereas the southern portion is dominated by forest. In both parts, significant urbanized areas exist.

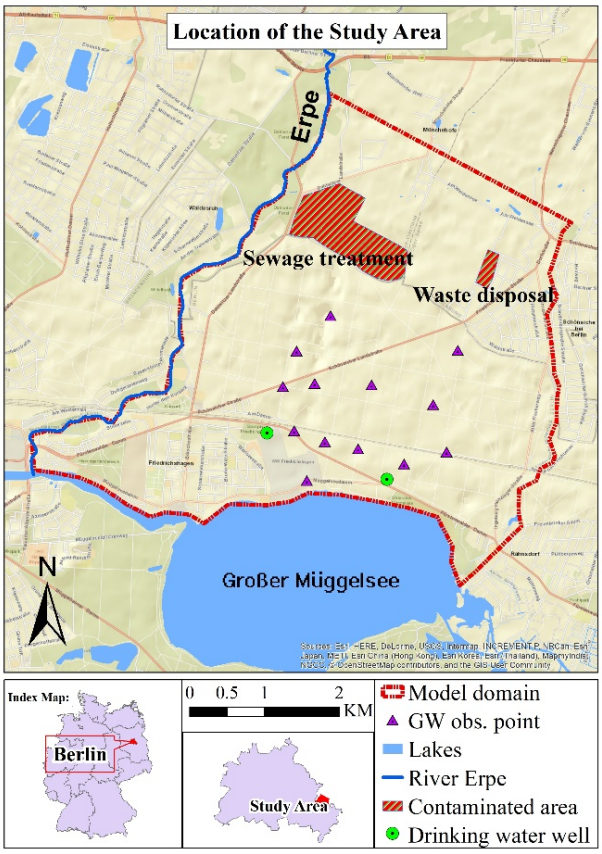

Figure 1. Study Domain of this study.

2.2. Data Preprocessing

The following information was used to build the model: Using ArcGIS, they underwent preprocessing: A shapefile called annual recharge describes regions (polygons) with varying groundwater recharge over time. A shapefile called average recharge identifies polygonal regions with dry, average, or wet groundwater recharge. The shapefile (points) "boreholes" describes drilling points with a sediment core, with each point's x, y, and vertical absolute positions (relative to a reference zero) and the material labeled in accordance with a laboratory sieving test, as well as the material's transmissive and pervious properties. A drinking water well is defined by a shapefile (points) that includes details such as the radius and pumping rate. Elevations is a shapefile (points) that displays the elevation of common geological properties and was created using surface survey and drilling data. With groundwater measurement stations, the shapefile (points) known as GW measuring

 doi:10.20944/preprints202209.0452.v1

describes the recorded groundwater level (average values). A shapefile called nitrate concentration contains details about the nitrate measurement sites and their associated values. topography rectified1 It displays the overall region and is a tiff file.

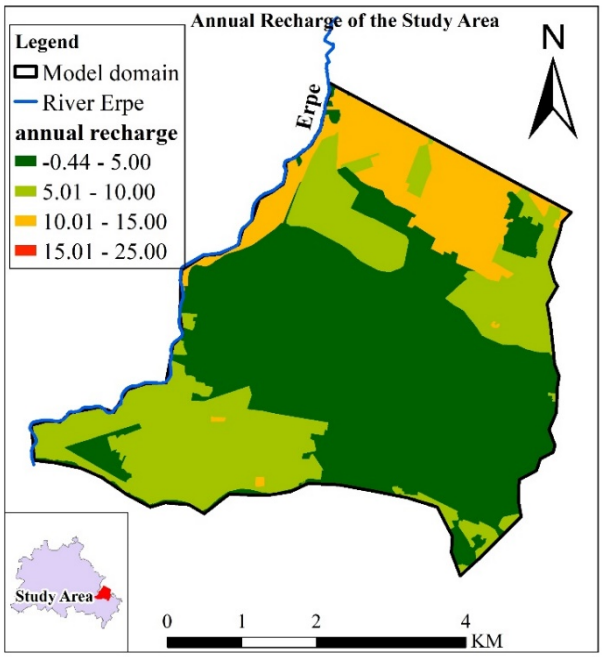

Figure 2. Map of the annual recharge of the study area.

As there are multiple rivers, streams and lakes in the region, their location can help to identify a suitable modeling domain. In Germany most waterbodies are feed by groundwater and thus their hydraulic head can help to define the boundary condition and modeling domain. The map of the annual recharge of the study area is shown in the Figure 2. River water is, same as groundwater subject to the gravitational forces and therefore generally follows the surface elevation. Where river and groundwater move parallel, the outer groundwater modeling domain can be delineated along the river, as they can be assumed to move parallel and thus be represented as an impermeable boundary. The remaining domain boundaries can be to be found by identifying stable groundwater isolines or waterbodies such as lakes that are well connected (same elevation as the groundwater level). At these boundaries, the Dirichlet boundary condition can be set, if no other information is known. The shapefiles describing the waterbodies and land-use were downloaded from the following link. In order to get the correct zone for the projection, the following website was used to get information: https://www.deineberge.de/Rechner/Koordinaten/Dezimal/43.796872,7.253723.

The well-connected river Spree and lake Müggelsee, which form the southern border, entirely govern the head along that border. These bodies of water have a significant link to the subterranean water. One option for a value for a first sort (Dirichlet) hydraulic head boundary condition is the constant lake water level of 32.1 m. The boundaries are formed by two minor rivers, the "Erpe" or the Neuenhagener Mühlenfließen (Erpe) on the western side and the "Fredersdorfer Mühlenfließen" on the eastern side. It was hypothesized that these minor creeks flow parallel to the GW because they roughly follow the groundwater flow direction and the surface contour.Under typical low flow circumstances, no water exchange over this boundary is anticipated, hence a no flow border condition can be assumed. Since there are no nearby natural boundary conditions, such as a water divide, a groundwater head contour line was employed, for example, a hydraulic

head of 46 m. Only along the same contour line does this border condition hold true.

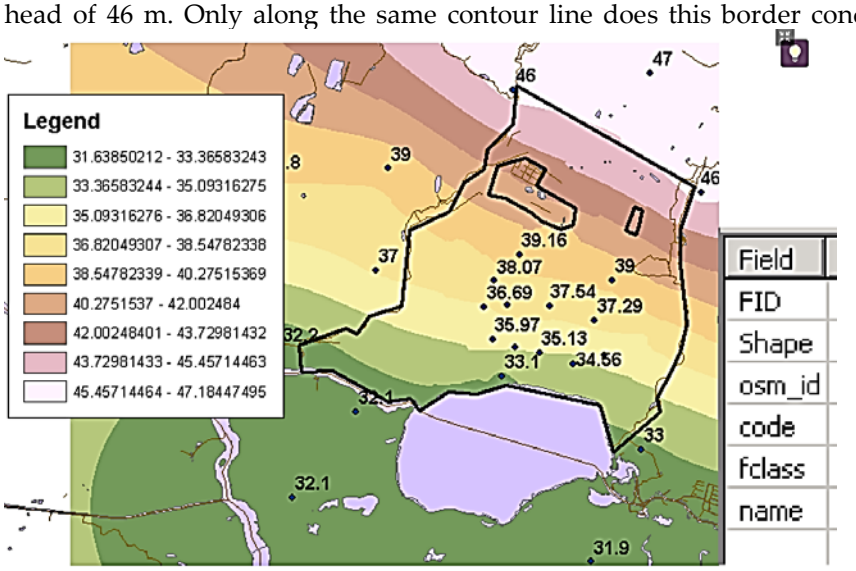

Figure 3. Observed groundwater level value along with locations and interpolated contour lines in the model domain.

The Groundwater measurement stations that are inside your modeling domain were located for the calibration (Figure 3). Contaminated area was also delineated in ArcGIS inside the model domain. Borehole data from bore hole shape file was used to plan the 3D conceptual design and hydrological structure of different systems of the model such as aquifer, aquitards, and aquiclude. Map of different soil types can be seen in the following figure. According to the soil properties, material properties (e.g., conductivity) can be determined.

2.3. FEFLOW Model Setup

At the beginning, a steady model was set and simulated to obtain the initial condition for the hydraulic head and pressure distribution for the transient model. The first step of the model set up in Feflow is the creation of super mesh. For creating super mesh, necessary maps are imported. All maps were prepared in shapefiles using ArcGIS. Shapefiles contains necessary polygons or poly points which feature the exact boundary of areas within the domain, the domain itself and wells. The calibration and sensitivity analysis can also be conducted using the steady model. Although the transient model was used for the calibration and sensitivity analysis due to slight modification in mesh quality. The transient model included mass transport of the mass within the contaminated area and transient data for the drinking water well pumps as well as a time series for the annual recharge. In the most straightforward scenario, the super mesh includes a specification of the outer model border. The position of pumping wells, the boundaries of regions with various qualities, or the courses of rivers are other geometrical aspects that may be taken into account while creating the finite-element mesh. The super mesh's provided polygons, lines, and points can also be utilized later to specify boundary constraints or material qualities. Three different sorts of features, such as polygons, lines, and points, may be found in a super mesh. The borders of the model region were defined using a polygon. The necessary polygons were directly loaded from the map shapefiles. Before generating the finite-element mesh, the well locations were also included in the super mesh. The domain polygon was separated into multiple aligned polygons with shared vertex and no gap between them to avoid overlapping using 'split polygon' function in Feflow.

Using split polygon tool, it was started with the first vertex at the outer edge of the domain near the contaminated areas then it was clicked at the edge of the contaminated area and traced the upper end of the shape continuing to the second contaminated area and finishing at the opposite edge of the domain. Again, it was started at the last point from the previous split and traced all the way back to the original vertex again finishing

 doi:10.20944/preprints202209.0452.v1

at the opposing site of the domain. At last, it was finalized by clicking enter. The super mesh was used to determine the outside border and other geometrical restrictions before creating the finite-element mesh. Advancing Front, Triangle, Grid Builder and Transport Mapping (Quadrilateral Mode only). Each of the mesh-generation algorithms has its specific property settings. The mesh generation is based on an approximate number of elements to be generated, either for the entire mesh or for each of the polygons. Mesh generation typically is an iterative process, changing the generator settings and element numbers until a satisfactory finite-element mesh is obtained. For improving the quality of mesh, obtuse angles in finite elements were avoided. The more obtuse the angle, the poorer the solution quality at the corresponding node. Keeping this in mind, obtuse angles of the triangles were removed by flipping edge technique. The transitions from the course to fine parts of the mesh were kept smooth. Fine mesh was accomplished to cover the physical processes in sufficient detail (e.g., around wells, in zones of contaminant movement and beside the river). Using Grid builder as a mesh-generating algorithm, 5000 elements were created in total. Local refinement was performed in well locations and contaminated areas. Delaunay Triangulation is an important aspect for the quality of mesh. Delaunay criteria violation was avoided using flipping edge technique or moving the nodes where necessary.

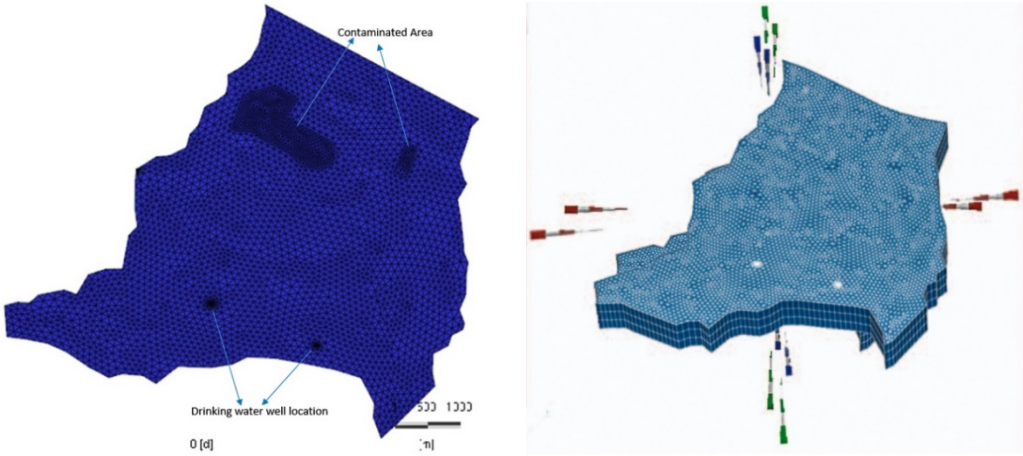

Figure 4. Model domain showing super mesh with high mesh resolution at the contaminated and drinking water well locations, 3D configuration.

Up until this point, we only took the model's top perspective into account and ignored its vertical orientation. This 2D geometry serves as the foundation for the creation of a multi-layered 3D model. A map-based interpolation is used to determine the top and bottom elevations of the layers (point-based data). Three geological strata were taken into consideration for the model in this study. The ground surface on top and an aquitard at the bottom restrict an upper aquifer. Below the aquitard lies a second aquifer that is covered by an unidentified low permeability unit of unknown thickness. This lower stratigraphic stratum is not included in the simulation since it is thought to be impenetrable. Layers are three-dimensional objects that often depict aquifers and aquitards, among other geological formations. Slices are the top- and bottom-model boundaries as well as the interfaces between layers. You may see that the vertical resolution for the transient model was later improved by adding an additional layer to the upper slice between the second and third slices at a distance of 0.1 meters. By regionalizing the elevation data found in map files, this raw geometry was given its actual shape. At first the elevation map (shapefile) was linked to the geometrical property of elevation of Feflow in the data panel. To regionalize the point data, specify Akima as interpolation method with the following properties, linear interpolation, 3 neighbors, Zero under or overshooting. The values of elevation were assigned to all nodes. In this same fashion, other necessary shape

 doi:10.20944/preprints202209.0452.v1

files were linked with their respective properties. The Problem Class page defines the FEFLOW model's primary type. Standard (saturated) groundwater flow equation (Darcy equation) was chosen. Steady state simulation for flow was selected for steady analysis. Unconfined aquifer was chosen under free surface problem class. The first slice of the model was changed to 'phreatic' and others was changed to 'dependent'. A residual water depth for unconfined layers of 0.05m was specified. The proper boundary conditions were used to compute the hydraulic head distribution between the upstream and downstream boundary. They were preserved in a very straightforward manner for the sake of simplicity. The head along the southern border is entirely under the administration of Lake Müggelsee. The value for a first sort (Dirichlet) hydraulic head boundary condition is the lake's water level of 32.1 m. In place of a natural boundary condition like a water split at the northern border (hydraulic head = 46 m), a head contour line was employed.On the other side, the model's western and eastern bounds are defined by two tiny rivers, the Fredersdorfer Mühlenfließen and the Neuenhagener Mühlenfließen. We infer that these severely congested streams serve as boundary streamlines because they generally correspond to the direction of groundwater flow. Since there should be no exchange of water across this barrier, a no-flow boundary condition is presumptive. Finally, two wells with a 1,000 m^3/d pumping rate and a radius of 0.2 m were placed in the model's southern region. These correspond to a huge number of genuine well fields. The wells were produced using a map, however the hydraulic head boundary criteria were manually input. All information needed for the material (elemental) properties were given in the Borehole shapefile. It can be used for linking the parameter to the corresponding material property in the data panel. Otherwise, in case of a homogenous value throughout the entire layer it is quick to select the entire layer and then assign the value manually. Material property namely conductivity (m/s) was for complete layer as follows in the beginning (Table).

Table 1. Layer components.

Components	Layer 1	Layer 2	Layer 3
In/Outflow on top/bottom	195mm/a	N/A	N/A
K_xx	N/A	2e-4m/s	1e-6m/s
K_yy	N/A	2e-4m/s	1e-6m/s
K_zz	N/A	2e-5m/s	1e-7m/s
Drain/Fillable Porosity	0.1	0.15	0.1

By interpolating data from field samples in the x direction for all slices, the hydraulic conductivity was determined. The map of borehole drilling points was linked with the conductivity in Feflow. For regionalizing the point data, Akima as interpolation method was specified with the properties such as Linear interpolation, 3 neighbors, zero under or overshooting and activate logarithmic in Feflow. 10% of the conductivity in x and y direction for the conductivity in z direction was used for all elements. Before running the file, the given observation points were added for calibration, by loading them into the maps file, and converting them into observation points. Finally, before running the steady model, mesh quality (max. interior angle, Delauney criterion, smoothing mesh, mesh refinement) was checked. For setting up the transient model, some modifications are required in the problem setting section of Feflow. Simulation time was adopted 7300 days for transient model and the fluid flow was considered as transient. The hydraulic head initial conditions have already been calculated from the basic steady model. Initial condition for mass distribution at the contaminated site were given from the map (shapefile) containing measured nitrate values at the contaminated site. The map was linked to the parameter namely mass concentration. For regionalization of the data inverse distance as data regionalization with 4 neighbors and an exponent of 2 was chosen. The nodes in the polygon delineating the contaminated area were selected and the values of contamination were assigned. A zero mg/l Dirichlet BC for the mass transport at the southern and northern boundary were selected. Minimum mass flow constraint was set to 0 g/d. Applying a set concentration is to be preferred over allowing polluted water to flow freely. Applying

 doi:10.20944/preprints202209.0452.v1

a constraint can be used to accomplish the dynamic modification of the mass transport boundary condition based on the flow direction. In this scenario, a constraint is employed to set a minimum or maximum value for the mass flow at a given concentration first type boundary condition. The restriction for this investigation is specified to exclusively apply the concentration boundary condition to inflowing water, limiting the mass flux to a minimum value of 0 g/d. The wells in this model have a time dependent pumping regime, which was loaded as a time series. Proper time series was imported in Feflow. As the annual rainfall data shows a significant variability during the simulated period, the groundwater recharge is assumed to be time-varying in the model. The file recharge_annual.shp contains the spatial distribution of the approximated recharge for annual periods each in a separate attribute field. Necessary parameter association was performed considering the time series. Porosity was considered to be 0.2, longitudinal dispersivity to be 70m and transverse dispersivity to be 7m. Finally, the simulation was performed keeping the record of process variable such as hydraulic conductivity, pressure head, mass concentration etc.

3. Results and Discussion

Chart of hydraulic head history was taken for the analysis the result quality. The values from the chart were imported to the MS excel. Different hydraulic head values at various observation points were loaded. A plot was made for observed hydraulic head vs simulated hydraulic head values at different observation points. Correlation between simulated & observed head value was found to be y = 1.289x - 2.7373 and the value of the correlation coefficient R2 to be 0.8916. R-squared is a statistical measure of how close the data are to the fitted regression line. In general, the higher the R-squared, the better the model line fits the data given. Calibration is not needed due to R2 being 0.8916 and this means that there is a good fit (perfect correlation has R^2=1) in the figure 7.

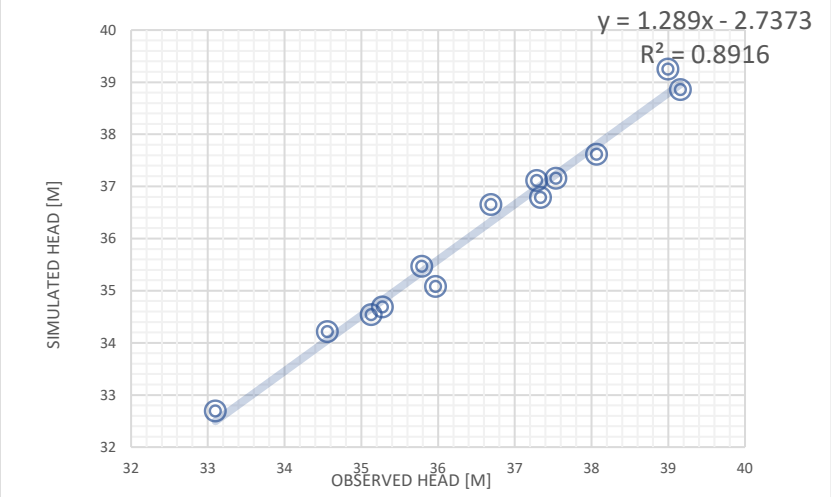

Figure 5. Correlation between simulated & observed head value.

3.1. Sensitivity Analysis

A sensitivity analysis has been carried out with the final model (transient) where the river Erpe was incorporated. The material property namely, transfer rate-in and transfer rate-out was used for the analysis. The base case is the final model having the river water level as boundary condition. Results such as hydraulic head, mass concentration and pressure were recorded and the impact of the change in the material property on these process variables were analyzed. The material property was changed in different percentage along the western border and the change in percentage of the process variables were observed as a result. An observation point was set to record the process variable (Figure 6) The process variables were observed at 7300 days (end of the simulation period).

Preprints (www.preprints.org) | NOT PEER-REVIEWED | Posted: 29 September 2022 doi:10.20944/preprints202209.0452.v1

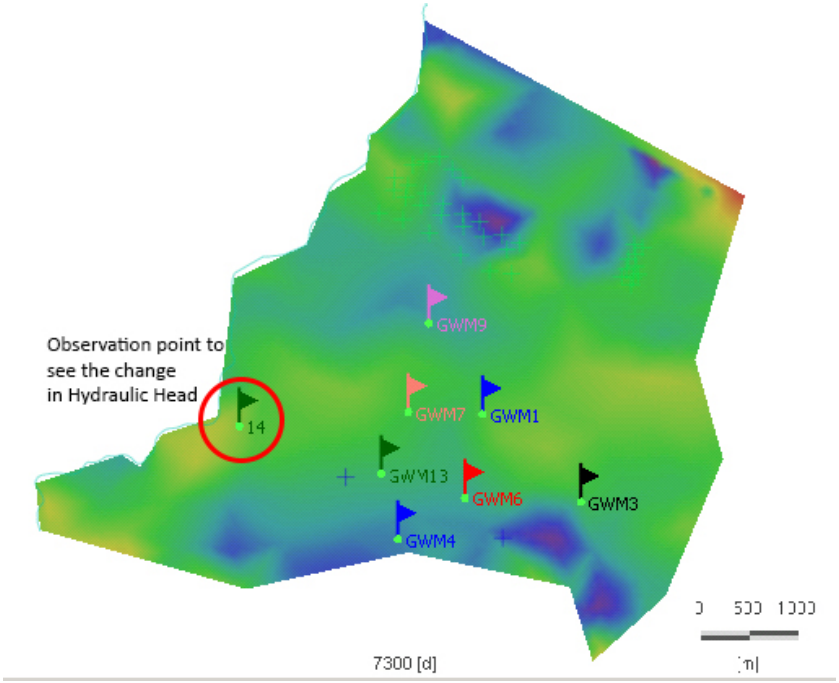

Figure 6. Observation location to see the change in hydraulic head.

Table 2. Variation of hydraulic head with changed material property (transfer rate in).

Head from Base Case (m)	Changed Head (m)	Change in Hydraulic Head (%)	Global Change in Material Property (%) (TRI)
35.5539	35.5535	−0.001	−100
35.5539	35.5535	−0.001	−50
35.5539	35.5538	−0.0003	50
35.5539	35.5537	−0.0006	100
35.5539	35.5536	−0.0008	150

Table 3. Variation of hydraulic head with changed material property (transfer rate out).

Head from Base Case (m)	Changed Head (m)	Change in Hydraulic Head (%)	Global Change in Material Property (%) (TRI)
35.5539	35.5541	0.001	−100
35.5539	35.5927	0.109	−50
35.5539	35.5539	0.0000	50
35.5539	35.5544	0.0014	100
35.5539	35.5541	0.0006	150

By analyzing the response in the process variable (hydraulic head) in the Table 2 and Table 3, it can be said that the model is not sensible to the changes in the Transfer Rate In and out and this property does not influence the simulation results. Due to no existence of a transfer boundary condition, no impact was found. It was found that, with the changed values in the property with different combination, the result was almost same in hydraulic head, mass concentration as well as pressure. Models were also set up for extremely higher values and for absolutely zero value of the transfer rate in and transfer rate out to check the model fails or not (Table 4). However, using the values mentioned in the following table, the model did not fail.

Table 4. Model scenario with high change in material property (transfer rate in and out).

Scenario Name (ID)	Transfer Rate in (l/d)	Percent Change (%)	Scenario Name (ID)	Transfer Rate Out (l/d)	Percent Change (%)	Comments

 doi:10.20944/preprints202209.0452.v1

SnScBase	200	n/a	SnScBase	800	n/a	Base scenario
SnSc1_TRI_Ex1	1200	500	SnSc1_TRO_Ex1	4800	500	Change in
SnSc1_TRI_Ex2	2200	1000	SnSc1_TRO_Ex2	8800	1000	Transfer rate
SnSc1_TRI_Ex3	4200	2000	SnSc1_TRO_Ex3	16800	2000	out

The sensitivity analysis on a different material property namely specific storage (compressibility) was also performed. The default value was 0.0001 1/m. Specific storage describes the change in volumetric water content in an aquifer induced per unit change in hydraulic head under saturated conditions. Along with specific yield, specific storage describes the storage properties of an aquifer. As in unconfined layers specific yield typically exceeds specific storage by far, the influence of this parameter in aquifers with phreatic surfaces is usually negligible. Different percentage change in specific storage was adopted. An observation point near the contamination area was set to record the change in process variables (hydraulic head, pressure, and mass transport). Different model was simulated using various specific storage (e.g. specific storage = 0.0001 (base case), 0.1, 1, 50, 100 1/m) (Figure 7). Most sensitive process variable was found to be the Mass Transport.

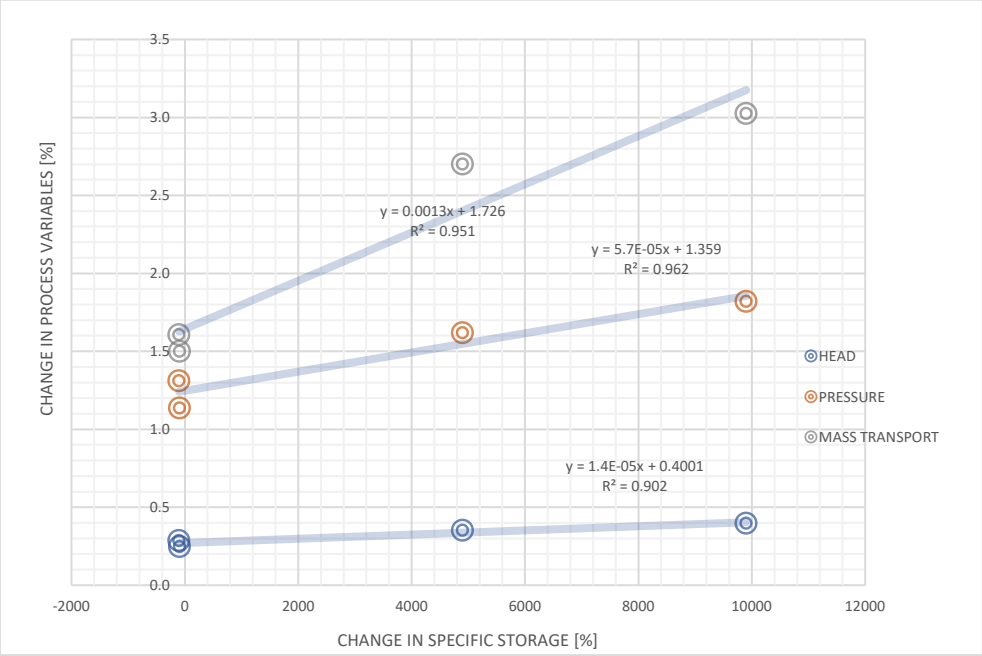

Figure 7. Impact of change in specific storage.

3.2. Flood Control Strategies

Three types of mitigation measures were considered. They are 1) installation of pumping well where the hydraulic level rises high (almost 1m below the surface level), 2) barrier and 3) drainage around the flood prone area (near urbane settlement around south-western part of the model. A pumping well having water withdrawal capacity of 2000 m3/d and a radius of 0.5 m was installed in the mitigation model scenario. A pumping well was found to be good solution for a local region. Pumping well cannot mitigate or lower the groundwater table over a wide region. For instance, the pumping well can be used for a small region likely 1kmx1km. The impact of pumping well on the hydraulic head is very localized. However, this is very effective technique to lower the hydraulic head over a small area.

On the other hand, drainage and barrier have also some influences over reducing the hydraulic head. Compared to pumping well, their effectiveness was found to be small. This can clearly be seen in the following figures where comparison of mitigated measure using pumping well and barrier are illustrated. Up to 1.5 m of reduction of hydraulic head

 doi:10.20944/preprints202209.0452.v1

can be achieved using pumping well whereas up to 200-300 cm of reduction of hydraulic head can be achieved by installing barrier (Figure 8 and Figure 9). Mitigation measure with drainage was also found to be very ineffective. Considering the bottom of the foundation level to be -1.5m for all structure on an average basis, pumping well was found to be most effective solution among barrier and drainage.

Moreover, the cost-benefit point of view also delineates that pumping well is more cost effective. Cost of construction of a well at a specific location is much lower than constructing a wall of up to 3m height or a drainage channel having up to 2.5m depth. On the other hand, approximately 935m long barrier or drainage channel had to be constructed to get some reduction in hydraulic head whereas only a single pumping well was seen enough reducing the hydraulic head over a small region.

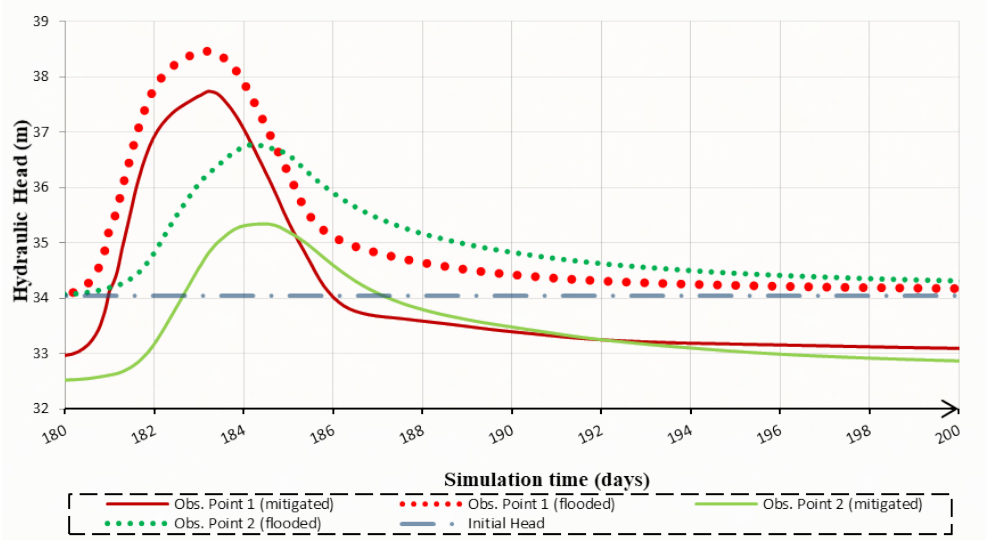

Figure 8. Comparison of Mitigated (well) and Flooding Scenario. Range of time period are considered where greater change in hydraulic head was observed (180-200days).

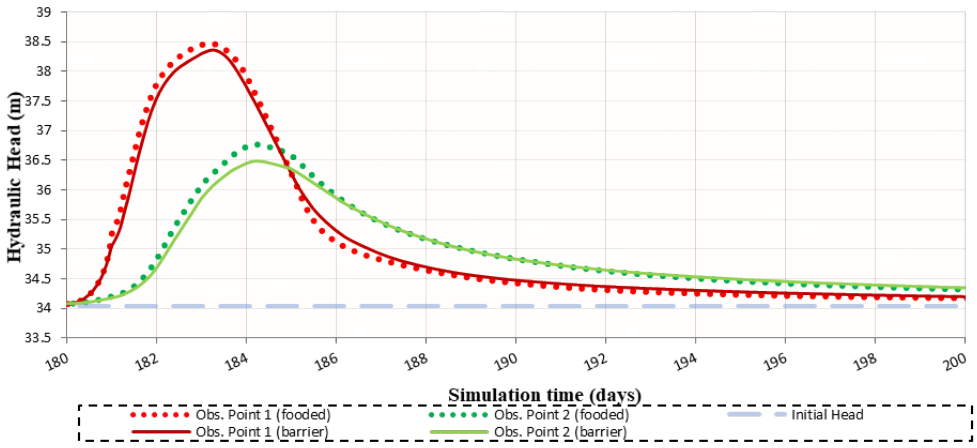

Figure 9. Comparison of Mitigated (barrier) and Flooding Scenario. Time period was considered to be 180-200 days.

 doi:10.20944/preprints202209.0452.v1

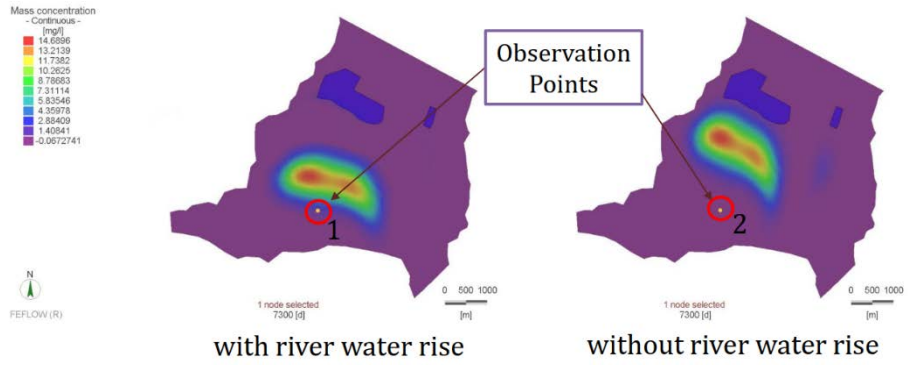

Figure 10. Spread of contaminant with and without considering the river Erpe.

Mass (nitrate) transport was varied due to the incorporation of the river water entrance as a boundary condition at the western port of the model (Figure 10). Mass transport was seen to be faster and traveled more path for 20 years (7300 years) of simulation compared to the case where river was not considered. For this reason, more nitrate concentration was observed at the observation point considering the river which is shown in the above figure. In spite of the fact that groundwater flooding due to river water rise is seldom, sometimes it becomes crucial when the river is flooded heavily. Groundwater flooding occurs as a result of water rising up from the underlying rocks or from water flowing from river. This tends to occur after long periods of sustained high rainfall. Higher rainfall means more water will infiltrate into the ground and cause the water table to rise above normal levels. When the house is knee-deep in water, groundwater flooding looks the same as river flooding. However, the flooding processes are different and management of the problem needs to reflect this. Groundwater flooding often persists long after river flooding has subsided. Even 'underground flooding' can affect infrastructure and services such as underground trains and sewers. When water reaches the surface, the destructive potential also rises. Flooded sewers can overflow causing contaminated water to emerge into streets, gardens and homes. Property can be damaged and people's lives can be turned upside down. Groundwater flooding is most likely to occur in low-lying areas underlain by permeable rocks (aquifers).

In this study domain, no groundwater overtopping of the surface was observed by the simulation of groundwater model using Feflow. Maximum hydraulic head was found over the urban settlement area situated at south-western part of the study domain. By subtracting the hydraulic head from the surface elevation groundwater depth was found and the minimum value was found to be approximately 1m below the surface level. This level can be crucial at the urban settlement area where lot of single storied buildings are situated. A pumping well was found to be more effective compared to barrier construction and drainage installment technique in both technically and cost-benefit point of view. A pumping well was found to be suitable in reducing hydraulic head locally thus lowering the groundwater level. Data preprocessing is a very important step for groundwater modelling in Feflow. Sufficient data is needed over the whole domain. Otherwise, inaccuracy may result in predicting the process variables over a long period due to greater interpolation. Material properties should be considered according to the soil profile data. There might be different kind of soil type existing in a single domain. However, uniform material groundwater flooding looks the same as river flooding. However, the flooding processes are different and management of the problem needs to reflect this. Groundwater flooding often persists long after river flooding has subsided. Even 'underground flooding' can affect infrastructure and services such as underground trains and sewers. When water reaches the surface, the destructive potential also rises. Flooded sewers can overflow causing contaminated water to emerge into streets, gardens and homes. Property can be damaged and people's lives can be turned upside down. Groundwater flooding is most likely to occur in low-lying areas underlain by permeable rocks (aquifers).

4. Conclusion

In this study domain, no groundwater overtopping of the surface was observed by the simulation of groundwater model using Feflow. Maximum hydraulic head was found over the urban settlement area situated at south-western part of the study domain. By subtracting the hydraulic head from the surface elevation groundwater depth was found and the minimum value was found to be approximately 1m below the surface level. This level can be crucial at the urban settlement area where lot of single storied buildings are situated. A pumping well was found to be more effective compared to barrier construction and drainage installment technique in both technically and cost-benefit point of view. A pumping well was found to be suitable in reducing hydraulic head locally thus lowering the groundwater level.

Data preprocessing is a very important step for groundwater modelling in Feflow. Sufficient data is needed over the whole domain. Otherwise, inaccuracy may result in predicting the process variables over a long period due to greater interpolation. Material properties should be considered according to the soil profile data. There might be different kind of soil type existing in a single domain. However, uniform material property was considered in our model scenario. Considering the borehole data, the number and thickness of aquifers was considered in the model. Due to difference in boundary conditions, the model result may vary significantly. Total time period was 20 years for the model. In this period of time, process variables such as hydraulic head, pressure head come to a steady state (similar to the initial condition). During the high precipitation, therefore the river flooding, change in the process variable was high. Spatial distribution of hydraulic head and spread of contamination were studied in a range of time period of 20 years. Due to the consideration of river water rise, GW flooding has been observed. The urban settlement located at the south-western side of the study area is flood prone. Considering the land use and the cost of different mitigation possibilities, local mitigation by a water pumping well at the urban settlement area was found to be most efficient.

Author Contributions: Conceptualization, R.K., M.A.A.M.; Methodology, R.K., M.A.A.M., M.M.S.Y.; Investigation, R.K., M.A.A.M., M.M.S.Y.; Formal Analysis, R.K.; Resources, R.K.; Data Preparation, R.K.; Writing-Original Draft Preparation, M.A.A.M., M.M.S.Y., R.K. Writing—Review and Editing, M.A.A.M, M.M.S.Y., R.K.; Visualization R.K., M.A.A.M., M.M.S.Y.; Project Administration. All authors have read and agreed to the published version of the manuscript.

Funding: This research received no external funding

Institutional Review Board Statement: Not applicable.

Informed Consent Statement: Not applicable.

Data Availability Statement: Data collected for the study can be made available upon request from the corresponding author.

Conflicts of Interest: The authors declare no conflict of interest.

References

1. Macdonald, D.; Dixon, A.; Newell, A.; Hallaways, A. Groundwater Flooding within an Urbanised Flood Plain. *Journal of Flood Risk Management* **2011**, *5*, 68–80, doi:10.1111/j.1753-318x.2011.01127.x.
2. Lu, C.; Ji, K.; Wang, W.; Zhang, Y.; Ealotswe, T.K.; Qin, W.; Lu, J.; Liu, B.; Shu, L. Estimation of the Interaction between Groundwater and Surface Water Based on Flow Routing Using an Improved Nonlinear Muskingum-Cunge Method. *Water Resources Management* **2021**, *35*, 2649–2666, doi:10.1007/s11269-021-02857-9.
3. Yazdan, M.M.S.; Ahad, M.T.; Kumar, R.; Mehedi, M.A.A. Estimating Flooding at River Spree Floodplain Using HEC-RAS Simulation. *Preprints* **2022**, 2022090410 (doi: 10.20944/preprints202209.0410.v1).
4. Mehedi, M.A.A.; Khosravi, M.; Yazdan, M.M.S.; Shabanian, H. Exploring Temporal Dynamics of River Discharge using Univariate Long Short-Term Memory (LSTM) Recurrent Neural Network at East Branch of Delaware River. *Preprints* **2022**, 2022090398 (doi: 10.20944/preprints202209.0398.v1).
5. Yazdan, M.M.S.; Khosravia, M.; Saki, S.; Mehedi, M.A.A. Forecasting Energy Consumption Time Series Using Recurrent Neural Network in Tensorflow . *Preprints* **2022**, 2022090404 (doi: 10.20944/preprints202209.0404.v1).
6. Kumar, C. Climate Change and Its Impact on Groundwater Resources. *RESEARCH INVENTY: International Journal of Engineering and Science* **2012**, *1*, 43–60.

7. Yazdan, M.M.S. Kumar, R.; Leung, S.W. The Environmental and Health Impacts of Steroids and Hormones in Wastewater Effluent, as Well as Existing Removal Technologies: A Review. *Ecologies* **2022**, *3*, 206–224, doi:10.3390/ecologies3020016.
8. Nemčić-Jurec, J.; Ruk, D.; Oreščanin, V.; Kovač, I.; Ujević Bošnjak, M.; Kinsela, A.S. Groundwater Contamination in Public Water Supply Wells: Risk Assessment, Evaluation of Trends and Impact of Rainfall on Groundwater Quality. *Applied Water Science* **2022**, *12*, doi:10.1007/s13201-022-01697-1.
9. Abd-Elaty, I.; Negm, A.; Hamdan, A.M.; Nour-Eldeen, A.S.; Zeleňáková, M.; Hossen, H. Assessing the Hazards of Groundwater Logging in Tourism Aswan City, Egypt. *Water* **2022**, *14*, 1233, doi:10.3390/w14081233.
10. Mehedi, M.A.A.; Yazdan, M.M.S. Automated Particle Tracing & Sensitivity Analysis for Residence Time in a Saturated Subsurface Media. *Liquids* **2022**, *2*, 72–84, doi:10.3390/liquids2030006.
11. Zurqani, H.A.; Al-Bukhari, A.; Aldaikh, A.O.; Elfadli, K.I.; Bataw, A.A. Geospatial Mapping and Analysis of the 2019 Flood Disaster Extent and Impact in the City of Ghat in Southwestern Libya Using Google Earth Engine and Deep Learning Technique. *Environmental Applications of Remote Sensing and GIS in Libya* **2022**, 205–226, doi:10.1007/978-3-030-97810-5_10.
12. Mehedi, M.A.A.; Reichert, N.; Molkenthin, F. Sensitivity Analysis of Hyporheic Exchange to Small Scale Changes in Gravel-Sand Flumebed Using a Coupled Groundwater-Surface Water Model Available online: https://meetingorganizer.copernicus.org/EGU2020/EGU2020-20319.html (accessed on 30 July 2022).
13. Moran, B.J.; Boutt, D.F.; McKnight, S.V.; Jenckes, J.; Munk, L.A.; Corkran, D.; Kirshen, A. Relic Groundwater and Prolonged Drought Confound Interpretations of Water Sustainability and Lithium Extraction in Arid Lands. *Earth's Future* **2022**, *10*, doi:10.1029/2021ef002555.
14. Ma, X.; Dahlke, H.; Duncan, R.; Doll, D.; Martinez, P.; Lampinen, B.; Volder, A. Winter Flooding Recharges Groundwater in Almond Orchards with Limited Effects on Root Dynamics and Yield. *California Agriculture* **2022**, *76*, 1–7.
15. Mehedi, M.A.A.; Yazdan, M.M.S.; Ahad, M.T.; Akatu, W.; Kumar, R.; Rahman, A. Quantifying Small-Scale Hyporheic Streamlines and Resident Time under Gravel-Sand Streambed Using a Coupled HEC-RAS and MIN3P Model. *Eng* **2022**, *3*, 276–300, doi:10.3390/eng3020021.
16. Basu, B.; Morrissey, P.; Gill, L.W. Application of Nonlinear Time Series and Machine Learning Algorithms for Forecasting Groundwater Flooding in a Lowland Karst Area. *Water Resources Research* **2022**, *58*, doi:10.1029/2021wr029576.
17. Kumar, C. An Overview of Commonly Used Groundwater Modelling Software. International Journal of AdvancedResearch in Science, Engineering and Technology **2019**, 6.
18. Ahmad M, Al Mehedi MA, Yazdan MMS, Kumar R. Development of Machine Learning Flood Model Using Artificial Neural Network (ANN) at Var River. *Liquids*. **2022**; 2(3):147-160. https://doi.org/10.3390/liquids2030010
19. Macdonald D.M.J., Bloomfield J.P., Hughes A.G., MacDonald A.M., Adams B. & McKenzie A.A. Improving the understanding of the risk from groundwater flooding in the UK. *Proceedings of the European Conference on Flood Risk Management*, Oxford, 30 September–2 October, **2008.**
20. Cobby D., Morris S., Parkes A. & Robinson V. Groundwater flood risk management: advances towards meeting the requirements of the EU floods directive. *J Flood Risk Manag* **2009**, 2, (2), 111–119. https://doi.org/10.1111/j.1753-318X.2009.01025.x
21. Pinault J.-L., Amraoui N. & Golaz C. Groundwater-induced flooding in macropore-dominated hydrological system in the context of climate changes. *Water Resour Res* **2005**, 41, 1029–1036. https://doi.org/10.1029/2004WR003169
22. Finch J.W., Bradford R.B. & Hudson J.A. The spatial distribution of groundwater flooding in a chalk catchment in southern England. *Hydrol Process* **2004**, 18, (5), 959–971. https://doi.org/10.1002/hyp.1340
23. Naji, L.; Tawfiq, M.; Jabber, A. Solve the Groundwater Model Equation Using Fourier Transforms Method Research Article. *Journal homepage: www.ijaamm.com International Journal of Advances in Applied Mathematics and Mechanics* **2017**, *5*, 2347–2529.
24. Pinder, G.F. An Overview of Groundwater Modelling. *Groundwater Flow and Quality Modelling* **1988**, 119–134, doi:10.1007/978-94-009-2889-3_7.
25. Yazdan, M.M.S.; Ahad, M.T.; Mallick, Z.; Mallick, S.P.; Jahan, I.; Mazumder, M. An Overview of the Glucocorticoids' Pathways in the Environment and Their Removal Using Conventional Wastewater Treatment Systems. *Pollutants* **2021**, *1*, 141–155, doi:10.3390/pollutants1030012.
26. Tepe, N.; Romero, M.; Bau, M. High-Technology Metals as Emerging Contaminants: Strong Increase of Anthropogenic Gadolinium Levels in Tap Water of Berlin, Germany, from 2009 to 2012. *Applied Geochemistry* **2014**, *45*, 191–197, doi:10.1016/j.apgeochem.2014.04.006.
27. Kuhlemann, L.; Tetzlaff, D.; Soulsby, C. Urban Water Systems under Climate Stress: An Isotopic Perspective from Berlin, Germany. *Hydrological Processes* **2020**, *34*, 3758–3776, doi:10.1002/hyp.13850.
28. Wise, D.L. *Bioremediation of Contaminated Soils*; CRC Press, 2000; ISBN 9780429078040.
29. García Revilla, M.R.; Martínez Moure, O. Wine as a Tourist Resource: New Manifestations and Consequences of a Quality Product from the Perspective of Sustainability. Case Analysis of the Province of Málaga. *Sustainability* **2021**, *13*, 13003, doi:10.3390/su132313003.
30. Richter, D.; Massmann, G.; Taute, T.; Duennbier, U. Investigation of the Fate of Sulfonamides Downgradient of a Decommissioned Sewage Farm near Berlin, Germany. *Journal of Contaminant Hydrology* **2009**, *106*, 183–194, doi:10.1016/j.jconhyd.2009.03.001.
31. Kinzelbach, W. Groundwater Modelling: An Introduction with Sample Programs in BASIC; Elsevier, 1986;

32. Kumar, C.P. "IJMSET Promotes Research Nature, Research Nature Enriches the World's Future" Modelling of Groundwater Flow and Data Requirements; 2015;
33. Ohara, N.; Steven Holbrook, W.; Yamatani, K.; Flinchum, B.A.; St. Clair, J.T. Spatial Delineation of Riparian Groundwater within Alluvium Deposit of Mountainous Region Using Laplace Equation. *Hydrological Processes* **2017**, *32*, 30–38, doi:10.1002/hyp.11395.
34. Ling, L.; Jian, C.; Haobo, N.; Li, L.; Leyi, Y.; Yaqiang, W. 基于 FEFLOW 的三维土壤-地下水耦合铬污染数值模拟研究 刘 玲，陈 坚，牛浩博，李 璐，殷乐宜，魏亚强 Numerical Simulation of Three-Dimensional Soil-Groundwater Coupled Chromium Contamination Based on FEFLOW. *Hydrogeology & Engineering Geology* **2022**, *49(1)*, doi:10.16030/j.cnki.issn.1000-3665.202102008.
35. Ashraf, A.; Ahmad, Z. Regional Groundwater Flow Modelling of Upper Chaj Doab of Indus Basin, Pakistan Using Finite Element Model (Feflow) and Geoinformatics. *Geophysical Journal International* **2008**, *173*, 17–24, doi:10.1111/j.1365-246x.2007.03708.x.
36. Yazdan, M.Md.S.; Ahad, M.T.; Jahan, I.; Mazumder, M. Review on the Evaluation of the Impacts of Wastewater Disposal in Hydraulic Fracturing Industry in the United States. *Technologies* **2020**, *8*, 67, doi:10.3390/technologies8040067.
37. Zhao, C.; Wang, Y.; Chen, X.; Li, B. Simulation of the Effects of Groundwater Level on Vegetation Change by Combining FEFLOW Software. *Ecological Modelling* **2005**, *187*, 341–351, doi:10.1016/j.ecolmodel.2004.10.019.
38. Diersch, H.-J.G. FEFLOW: Finite Element Modeling of Flow, Mass and Heat Transport in Porous and Fractured Media; Springer Science & Business Media, 2013;
39. Rahaman, A.; Md, M.; Yazdan, S.; Noor, F. ESTABLISHMENT of CO-RELATION between REMOTE SENSING BASED TRMM DATA and GROUND BASED PRECIPITATION DATA in NORTH-EAST REGION of BANGLADESH Deep Convection for Thunderstorm: CAPE and Shear Analysis in Present and Future Climate View Project Seven River Dredging Project: Case of Old Brahmaputra River View Project; 2014;
40. Kaur, B.; Binns, A.; Sandink, D.; Gharabaghi, B.; McBean, E. Reducing the Risk of Basement Flooding through Building- and Lot-Scale Flood Mitigation Approaches: Performance of Foundation Drainage Systems. *Lecture Notes in Civil Engineering* **2022**, 471–477, doi:10.1007/978-981-19-1065-4_39.
41. Tamim, B.; Hossain, A.; Ahmed, T.; Aktar; Fida, M.; Khan, A.; Islam, S.; Yazdan, M.; Noor, F.; Rahaman, A. *CLIMATE CHANGE IMPACTS on WATER AVAILABILITY in the MEGHNA BASIN*; 2015;
42. Humnicki, W.; Krogulec, E.; Małecki, J.; Szostakiewicz-Hołownia, M.; Wojdalska, A.; Zaszewski, D. Groundwater impact assessment of Lake Czorsztyn after 25 years of its operation. *Archives of Environmental Protection*, **2022**; 65-78, DOI 10.24425/aep.2022.140767.